Aminoalkyl-Substituted Indenyl−Nickel Compounds: Tuning Reactivities as a Function of the Pendant, Hemilabile Moiety

Laurent F. Groux and Davit Zargarian*

Département de Chimie, Université de Montréal, Montréal, Québec, Canada H3C 3J7

Received April 2, 2003

Indenyl ligands bearing three different aminoalkyl substituents have been used to prepare the complexes (Ind∧NR_2)Ni(PPh_3)Cl (Ind∧NR_2 = 2-(1-indenylmethyl)pyridine (**1**), *N*-(1-indenylethyl)pyrrolidine (**2**), and *N*-(1-indenylethyl)diisopropylamine (**3**)). The solution NMR spectra of complexes **1** and **2** point to the existence of a dynamic process involving the reversible coordination of the pendant amine moieties to the Ni center, but no N−Ni interaction is evident in complex **3**. Abstraction of Cl^- from the neutral precursors **1**−**3** yields the corresponding cationic derivatives [(η^3:η^1-Ind∧NR_2)Ni(PPh_3)]$^+$ (**4**−**6**) wherein the amino tether is chelated to the nickel center. Complexes **1**−**5** have been isolated and fully characterized by multinuclear NMR spectroscopy and, in the case of **1** and **4**, by single-crystal X-ray diffraction studies. The isolation of complex **6** is complicated by its partial conversion to the bis(phosphine) derivative [{η^3:η^0-IndCH_2CH_2N(*i*-Pr)$_2$}Ni(PPh_3)$_2$]$^+$ (**7**). Studies on the displacement of the chelating amine moiety in **4** and **5** by dppe, PPh_3, and pyridine showed the pyridine moiety to be the least labile. Cyclic voltammetry studies have shown that the reduction potentials of the complexes vary as a function of the Ni−N interaction, the complexes bearing the NMe_2 moieties showing the strongest resistance to reduction. Olefin polymerization reactions also showed that the nature of the N-moiety has a considerable influence on the catalytic reactivity of the cationic complexes.

Introduction

The cyclopentadienyl ligand (Cp) and its congeners such as the indenyl (Ind) have played an important role in the development of organometallic chemistry. One attractive feature of these ligands is the ease with which their steric and electronic properties can be modified by the judicious introduction of diverse substituents. The versatility of Cp-type ligands can be further enhanced when their substituents bear coordinating moieties. For instance, the ligands Cp∧NR_2 (∧ denotes the tether that links the amine moiety to the Cp ring) are known to impart many interesting properties to their complexes, including superior catalytic reactivities, stabilization of otherwise unstable species, changing solubility properties, introducing chirality, and so on.[1] Although a wide variety of complexes bearing Cp∧NR_2 ligands are known for most transition metals, relatively few derivatives of group 10 metals have been reported[2] and little is known of their reactivities.

The above considerations and our long-standing interest in the chemistry of nickel indenyl complexes led us to study the reactivities of Ni complexes bearing the ligands Ind∧NR_2. In earlier reports, we have described the structures and reactivities of the neutral complexes (Ind$(CH_2)_n$NRR′)NiL(X) (n = 2−4; NRR′ = NH(*t*-Bu), NH(PhCH_2), NH_2, NMe_2; L = PPh_3, PCy_3, PMe_3; X = Cl, I, Me, Bu)[3] and the cationic complex [(η^3:η^1-Ind$(CH_2)_2$-NMe_2)Ni(PPh_3)]$^+$.[4] These studies showed that using the ligand Ind$(CH_2)_2NMe_2$ offers an important advantage over the nonfunctionalized Ind ligands; namely, the presence of a hemilabile N→Ni coordination in complexes incorporating this ligand prevents the formation of the catalytically inert bis(phosphine) derivatives [IndNi$(PR_3)_2$]$^+$, thereby improving the catalytic activities of the cationic complexes. Indeed, even when the amine moiety is not chelated, its proximity to the Ni center seems to have a marked influence over the course of the catalytic reactions and the nature of their products. These findings prompted us to prepare new complexes featuring Ind∧NR_2 ligands with different coordinating properties in order to investigate further the role played by the amine moiety on the stability and reactivities of these complexes.

The present article describes the preparation and characterization of a new series of neutral and cationic nickel complexes bearing the ligands 2-(1-indenylmeth-

(1) For reviews of this topic see: (a) Müller, C.; Vos, D.; Jutzi, P. *J. Organomet. Chem.* **2000** *600*, 127. (b) Jutzi, P.; Redeker, T. *Eur. J. Inorg. Chem.* **1998**, 663. (c) Jutzi, P.; Siemeling, U. *J. Organomet. Chem.* **1995**, *500*, 175. (d) Jutzi, P.; Dahlaus, J. *Coord. Chem. Rev.* **1994**, *137*, 179.

(2) (a) Oberbeckmann, N.; Merz, K.; Fischer, R. A. *Organometallics* **2001**, *20*, 3265. (b) Segnitz, O.; Winter, M.; Merz, K.; Fischer, R. A. *Eur. J. Inorg. Chem.* **2000**, 2077. (c) Hoffmann, H.; Fischer, R. A.; Antelmann, B.; Huttner, G. *J. Organomet. Chem.* **1999**, *584*, 131. (d) Weiss, J.; Frank, A.; Herdweck, E.; Nlate, S.; Mattner, M.; Fischer, R. A. *Chem. Ber.* **1996**, *129*, 297. (e) Fischer, R. A.; Nlate, S.; Hoffmann, H.; Herdweck, E.; Blumel, J. *Organometallics* **1996**, *15*, 5746. (f) Nlate, S.; Herdweck, E.; Fischer, R. A. *Angew. Chem., Int. Ed. Engl.* **1996**, *35*, 1861. (g) Jutzi, P.; Redeker, T.; Neumann, B.; Stammler, H.-G. *J. Organomet. Chem.* **1995**, *498*, 127.

(3) Groux, L. F.; Bélanger-Gariépy, F.; Zargarian, D.; Vollmerhaus, R. *Organometallics* **2000**, *19*, 1507.

(4) (a) Groux, L. F.; Zargarian, D. *Organometallics* **2001**, *20*, 3811. (b) Groux, L. F.; Zargarian, D.; Simon, L. C.; Soares, J. B. P. *J. Mol. Catal. A Chem.* **2003**, *193*, 51.

10.1021/om030241q CCC: $25.00
Publication on Web 06/21/2003

Scheme 1

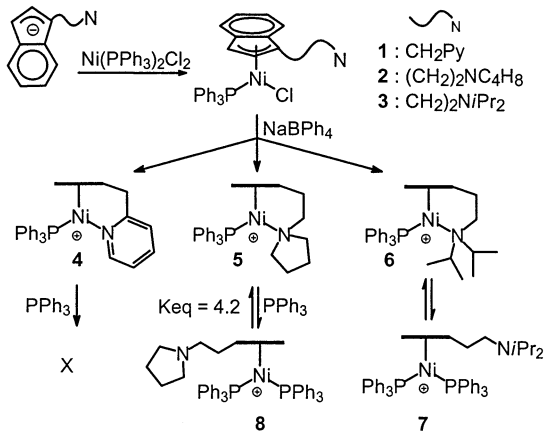

Scheme 2

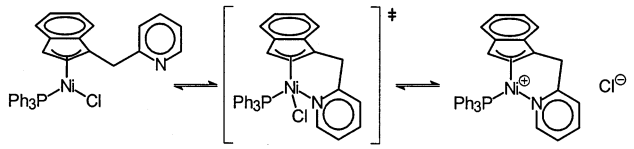

yl)pyridine, *N*-(1-indenylethyl)pyrrolidine, and *N*-(1-indenylethyl)diisopropylamine. NMR studies were carried out to evaluate the interaction of the tethered amine moiety with the Ni center in the neutral compounds and study the reaction of nucleophiles with the cationic compounds. Reactivity studies have also shown that the cationic complexes can convert styrene into poly(styrenes); both the polymerization activities of the precatalysts and the molecular weights of the resulting polymers depend on the nature of Ni−N interaction.

Results and Discussion

The amino-functionalized Ind ligands were prepared according to literature procedures[5] by adding the appropriate Cl∧NR_2 to an Et_2O solution of LiInd, followed by standard aqueous workup. Subsequent deprotonation of the resultant Ind∧NR_2 and reaction with Ni(PPh_3)$_2$-Cl_2 gave the desired products (Scheme 1). In the process of isolating these complexes, we found that their solubilities varied greatly with the type of pendant amine moiety: whereas the complex (IndCH_2-*o*-Py)Ni(PPh_3)-Cl (**1**) readily precipitated from concentrated Et_2O solutions, the analogous complexes bearing the ligands *N*-(1-indenylethyl)pyrrolidine (**2**) and *N*-(1-indenylethyl)diisopropylamine (**3**) needed multiple recrystallizations from less polar solutions.

Solution NMR studies of the neutral complexes **1**−**3** revealed a dynamic process involving the reversible coordination of the amine moieties in complexes **1** and **2** to the Ni center (Scheme 2), but no such interaction was detected in complex **3**. As will be described in detail later, the Ni−N interaction in **1** and **2** is stronger at higher temperatures, while at lower temperatures the spectral features of these complexes resemble those of analogous complexes that do not bear functionalized substituents on Ind.

The solid state structure of complex **1** has been studied by X-ray crystallography. Table 1 lists the crystal data and the details of data collection and structure refinement, while Table 2 contains selected structural parameters. The ORTEP diagram of **1** (Figure 1) shows that the pyridine moiety is oriented away from

Table 1. Crystal Data, Data Collection, and Structure Refinement of 1 and 4

	1	**4**
formula	$C_{33}H_{27}ClNPNi$	$C_{57}H_{47}BNPNi\cdot CH_2Cl_2$
mol wt	562.69	931.37
cryst color, habit	dark red, block	dark red, block
cryst dimens, mm	0.25 × 0.23 × 0.14	0.28 × 0.27 × 0.11
symmetry	triclinic	monoclinic
space group	$P\bar{1}$	$P2_1/c$
a, Å	9.196(3)	10.4368(1)
b, Å	12.924(5)	21.0121(2)
c, Å	12.943(3)	21.7137(2)
α, deg	85.99(3)	90
β, deg	73.28(2)	96.340(1)
γ, deg	70.72(3)	90
volume, Å^3	1390.1(8)	4732.67(8)
Z	2	4
D(calcd), g cm^{-1}	1.3443	1.3072
diffractometer	Nonius CAD-4	Bruker AXS SMART 2K
temp, K	293(2)	223(2)
λ (Cu Kα), Å	1.54178	1.54178
μ, mm^{-1}	2.595	2.247
scan type	*ω*/2*θ* scan	*ω* scan
θ_{max}, deg	69.91	72.96
h,*k*,*l* range	$-11 \le h \le 11$ $-15 \le k \le 15$ $-15 \le l \le 15$	$-12 \le h \le 11$ $-25 \le k \le 25$ $-26 \le l \le 26$
no. of reflns used ($I > 2\sigma(I)$)	2892	6288
abs corr	integration ABSORB	multiscan SADABS
T(min, max)	0.4649, 0.7327	0.1816, 0.8306
$R[F^2>2\sigma(F^2)]$, $wR(F^2)$	0.0441, 0.0801	0.0508, 0.1221
GOF	0.979	1.041

Table 2. Selected Bond Distances (Å) and Angles (deg) for 1 and 4

	1	**4**
Ni−P	2.1847(13)	2.2006(7)
Ni−(Cl or N)	2.1784(13)	1.949(2)
Ni−C1	2.132(3)	2.023(2)
Ni−C2	2.071(4)	2.063(3)
Ni−C3	2.037(4)	2.095(3)
Ni−C3A	2.308(4)	2.325(2)
Ni−C7A	2.352(2)	2.280(2)
C1−C2	1.400(4)	1.421(4)
C2−C3	1.413(5)	1.401(4)
C3−C3A	1.457(5)	1.457(4)
C3A−C7A	1.416(5)	1.417(3)
C7A−C1	1.450(4)	1.470(3)
C1−C8	1.504(4)	1.481(3)
Δ(M−C)[§]	0.25	0.24
C1−Ni−(Cl or N)	95.83(11)	83.61(9)
P− Ni−(Cl or N)	97.10(5)	106.51(6)
P− Ni−C3	101.16(12)	103.19(8)
C1−Ni−C3	65.98(14)	67.24(10)
C3−Ni−(Cl or N)	161.73(11)	150.29(10)
P−Ni−C1	165.54(10)	166.58(8)
N−C9−C8	116.4(4)	116.4(2)
C1−C8−C9	109.7(3)	109.8(2)
HA[a]	10.1(5)	11.48(14)
FA[a]	8.8(4)	8.10(13)

[a] Δ M−C)= $^1/_2${(M−C3a + M−C7a) − (M−C1 + M−C3)}; HA = angle between C1/C2/C3 plane and C1/C3/C3A/C7A plane; FA = angle between C1/C2/C3 plane and C3A/C4/C5/C6/C7/C7A plane.

(5) (a) Döhring, A.; Göhre, J.; Jolly, P. W.; Kryger, B.; Rust, J.; Verhovnik, G. P. J. *Organometallics* **2000**, *19*, 388. (b) Blais, M. S.; Chien, J. C. W.; Rausch, M. D. *Organometallics* **1998**, *17*, 3775. (c) Ziniuk, Z.; Goldberg, I.; Moshe, K. *J. Organomet. Chem*. **1997**, *545*−*546*, 441.

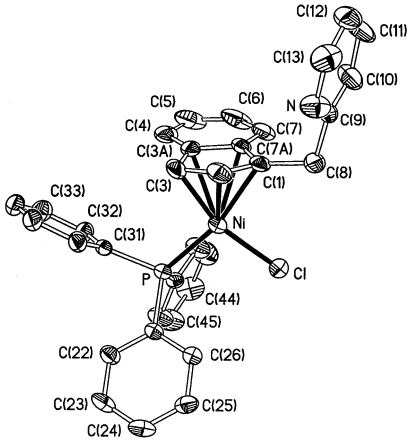

Figure 1. ORTEP view of complex **1**. Thermal ellipsoids are shown at 30% probability, and hydrogen atoms are omitted for clarity.

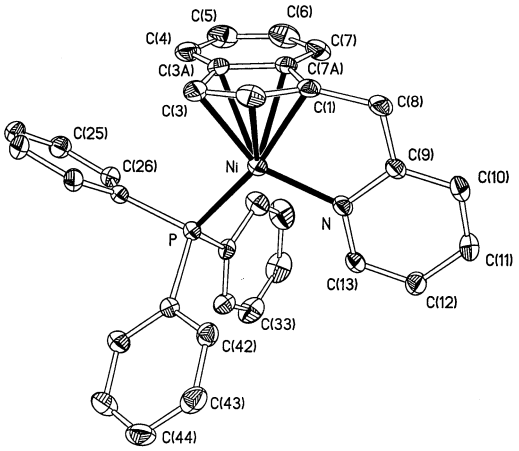

Figure 2. ORTEP view of complex **4**. Thermal ellipsoids are shown at 30% probability, and hydrogen atoms and the counterion (BPh_4) are omitted for clarity.

the Ni center and does not coordinate to it; the same observation was made for the previously studied complex (Ind-$CH_2CH_2NMe_2$)Ni(PPh_3)Cl.[3] In this sense, the solid state structure of these complexes represents their low-temperature solution behavior. The plane containing P, Cl, and Ni is perpendicular to the Ind ligand, which adopts an intermediate hapticity (Δ(M−C) = 0.25 Å);[6] hence, the overall geometry around the Ni center can be described as intermediate between a two-legged piano stool (assuming η^5-Ind) and square planar (assuming η^3-Ind). As anticipated on the basis of the relative trans influences of PPh_3 and Cl ligands, the Ni−C3 bond length is significantly shorter (by >20σ) than the Ni−C1 distance; therefore, the Ind hapticity can be more accurately described as ($\eta^5 \leftrightarrow \eta^1$:$\eta^2$).[7] The Ni−P, Ni−Cl, and C−C distances in complex **1** are similar to those found for the analogous complexes bearing nonfunctionalized Ind substituents.[8]

Reacting complex **1** or **2** with excess $NaBPh_4$ in CH_2Cl_2 gave the corresponding cationic complex **4** or **5**, respectively, in ca. 60% yield (Scheme 1). The $^{31}P\{^1H\}$ NMR spectra of the products showed new singlet resonances consistent with the coordination of only one PPh_3 to each Ni center, while the ^1H NMR spectra showed downfield shifts for the H3 signals (to ca. 4.0 ppm). Our previous studies showed that the conversion of (Ind$(CH_2)_2NMe_2$)Ni(PPh_3)Cl to [η^3:η^1(Ind$(CH_2)_2NMe_2$)-Ni(PPh_3)]$^+$ engendered similar changes in the NMR spectra;[3,4a] by analogy, we concluded that the amine moieties in **4** and **5** are chelated to the Ni center. This assertion was confirmed by the results of X-ray diffraction studies of complex **4** (vide infra).

In the case of complex **3**, abstraction of Cl^- gave both the anticipated N-chelated cation [(η^3:η^1-IndCH_2CH_2N(*i*-Pr)$_2$Ni(PPh_3)]$^+$ (**6**) and the bis(phosphine) cation [(η^3:η^0-IndCH_2CH_2N(*i*-Pr)$_2$Ni(PPh_3)$_2$]$^+$ (**7**) (Scheme 1). These species were identified on the basis of the $^{31}P\{^1H\}$ NMR spectrum of the reaction mixture, as follows. Complex **6** displayed a singlet resonance at 29.3 ppm, similar to the corresponding signal for complex **5** (30.3 ppm), whereas complex **7** gave rise to two AB doublets (36.5 and 32.1 ppm, $^2J_{P-P}$ = 25 Hz), which are virtually identical to the corresponding signals for [(1-Me-Ind)-Ni(PPh_3)$_2$]$^+$ (35.8 and 32.5 ppm, $^2J_{P-P}$ = 25 Hz),[9] suggesting that a second PPh_3 ligand is coordinated to the Ni center instead of the N(*i*-Pr)$_2$ moiety. This assignment was also corroborated by the fact that when excess PPh_3 was added to the mixture of **3** and $NaBPh_4$, the main product (>90%) was **7**. Complexes **6** and **7** interconvert in solution (Scheme 1), which prevented us from isolating pure **6** or **7**; this behavior is presumably caused by the large steric bulk of the (*i*-Pr)$_2$N moiety in **3** that hinders the N→Ni coordination.

Suitable single crystals of **4** were obtained from a cold CH_2Cl_2/Et_2O solution of this complex and subjected to an X-ray diffraction analysis. Crystal data and details of data collection and structure refinement are presented in Table 1, selected structural parameters are listed in Table 2, and an ORTEP diagram is shown in Figure 2. The overall geometry in **4** is very similar to that of complex **1**, but chelation of the pyridine moiety alters some parameters. For instance, the Ni−C1 distance is reduced by more than 0.1 Å on going from **1** to **4** despite the greater trans influence of PPh_3. The chelation also results in a smaller C1−Ni−N angle in **4** (ca. 84°) compared to the corresponding C1−Ni−Cl angle in **1** (ca. 96°). The Ind ligand also appears to be more tightly bound to the cationic center in **4**, as indicated by the generally shorter Ni−C distances. The Ni−N distance is 0.1 Å shorter than the average Ni−N distance found in the literature.[10] On the other hand, the Ni−P distance in **4** is longer by about 0.016 Å (ca. 20σ) compared to the neutral **1**; this is presumably because the Ni center becomes a harder Lewis acid upon ionization, thus being less compatible with the soft Lewis base PPh_3.

Comparing the main structural features of **4** and its analogue [(η^3:η^1-Ind$CH_2CH_2NMe_2$)Ni(PPh_3)]$^+$ shows that

(6) For a definition of the slip parameter Δ(M−C) see the footnotes of Table 2; for a discussion of its values in various Ind complexes see these reports: (a) Baker, R. T.; Tulip, T. H. *Organometallics* **1986**, *5*, 839. (b) Westcott, S. A.; Kakkar, A.; Stringer, G.; Taylor, N. J.; Marder, T. B. *J. Organomet. Chem.* **1990**, *394*, 777.

(7) Zargarian, D. *Coord. Chem. Rev.* **2002**, *233−234*, 157.

(8) (a) Huber, T. A.; Bayrakdarian, M.; Dion, S.; Dubuc, I.; Bélanger-Gariépy, F.; Zargarian, D. *Organometallics* **1997**, *16*, 5811. (b) Huber, T. A.; Bélanger-Gariépy, F.; Zargarian, D. *Organometallics* **1995**, *14*, 4997.

(9) Vollmerhaus, R.; Bélanger-Gariépy, F.; Zargarian, D.; *Organometallics* **1997**, *16*, 4762.

(10) A search using ConQuest (v 1.4, CCDC 2002) gave an average Ni−N distance of 2.054 Å when N = 2-(alkyl)pyridine.

Table 3. Electrochemical and NMR Data for Complexes 1−5 and Related Derivatives[a]

		^{1}H (ppm)				
	^{31}P{^{1}H} (ppm)	H2	H3	H4	E_{Red} (V obs)	E_{Red} (V vs SCE)
1[b]	30.6	6.43	3.22	6.05	−1.65	−1.36
2[c]	30.7	6.60	3.50	6.04	−1.64	−1.34
3[d]	30.8	6.60	3.43	6.10	−1.64	−1.34
(IndCH$_2$CH$_2$NMe$_2$)Ni(PPh$_3$)Cl[d]	30.8	6.70	3.42	6.11	−1.70	−1.41
(1-Me-Ind)Ni(PPh$_3$)Cl[c]	31.2	6.50	3.52	6.03		−1.26
4[e]	34.6	6.93	4.06	6.10	−1.34	−1.05
5[c]	30.3	6.80	3.97	5.50	−1.37	−1.08
[(η^3,η^1-Ind(CH$_2$)$_2$NMe$_2$)Ni(PPh$_3$)]$^{+}$[c]	29.1	6.78	3.94	5.54	−1.45	−1.16
(1-Me-Ind)Ni(PPh$_3$)$_2$]$^{+}$[c]	36.5, 32.9	6.27	4.79	6.05		−1.24

[a] All electrochemical studies were conducted in acetonitrile solutions and the NMR spectra are in the following solvents. [b] Toluene-d_8 −40 °C. [c] $CDCl_3$. [d] C_6D_6. [e] CD_2Cl_2.

the Ni−N distance is shorter and the overall Ni−Ind interaction is somewhat stronger in complex **4**, while the Ni−P distances are quite similar (within 3σ). These observations seemed to suggest that the Ni−N bond in **4** might be less labile, which is supported by the results of ligand substitution reactions (vide infra). The stronger Ni−N and Ni−Ind interactions seemed to suggest also that the Ni center in **4** should be more electron rich, but this was not borne out by the results of our electrochemical measurements (vide infra); as will be described later, these apparently contradictory observations can be reconciled by invoking Ni→N π-back-bonding in **4**.

Solution Behavior of the Neutral Complexes. The solution NMR spectra of the neutral complexes **1**−**3** have been compared to those of other IndNi compounds in order to determine whether the amine moiety in **1**−**3** is involved in N→Ni interactions (Table 3). Among the complexes examined, the most straightforward spectra were obtained for complex **3**, which displayed room-temperature spectral features similar to those of the complexes bearing nonfunctionalized Ind ligands.[7] For example, the ^{31}P{^{1}H} NMR spectrum of this complex showed a singlet resonance at 30.8 ppm, and the ^{1}H NMR spectrum showed the anticipated signals at ca. 6.60 and 3.50 ppm for H2 and H3, respectively, of the Ind ligand (numbering scheme shown in the ORTEP diagram, Figure 1). According to these spectra, little or no N→Ni interaction takes place in **3**, presumably because of the steric bulk of the (*i*-Pr)$_2$N moiety. In contrast, the amine moieties in complexes **1** and **2** reversibly coordinate to the Ni center, as inferred from their NMR spectral features described below.

The low-temperature ^{1}H, ^{31}P{^{1}H}, and ^{13}C{^{1}H} NMR spectra of complexes **1** and **2** displayed the requisite signals characteristic of the complexes bearing nonfunctionalized Ind ligands. Thus, the low-temperature ^{31}P{^{1}H} NMR spectra of these complexes (ca. − 40 °C, $CDCl_3$ or toluene-d_8) showed a singlet resonance at ca. 30−31 ppm, while the ^{1}H NMR spectra showed all the anticipated signals (e.g., 6.4−6.6 ppm for H2 and 3.2−3.4 ppm for H3). Warming the samples resulted in a gradual disappearance of all the signals, which occurred at around room temperature for complex **1** and at 40−50 °C for complex **2**. That this spectral bleaching is not caused by a thermal decomposition is evident from the observation that subsequent cooling of the sample restored all the original signals. By analogy with the previously studied complex (IndCH$_2$CH$_2$NMe$_2$)Ni(PPh$_3$)Cl, which shows a similar spectral behavior,[3] we conclude that complexes **1** and **2** are also subject to a dynamic process involving the reversible coordination of the amine moiety to the Ni center. The compound dominant at the low-temperature regime can be represented by the solid state structure of this complex (Figure 1), in which no N→Ni interaction is evident. This was confirmed by the room-temperature CP-MAS NMR spectrum of a solid sample of complex **1**, which showed signals similar to those of complexes bearing nonfunctionalized susbtituents on Ind.

The high-temperature NMR spectra were studied next in search of clues on the identity of the species featuring N→Ni chelation. In the case of complex **2**, even the highest temperature accessible to us (ca. 100 °C) did not drive the dynamic process beyond the coalescence point; as a result, we were unable to directly observe the species formed by the coordination of the pyrrolidine moiety. On the other hand, the dynamic process involving complex **1** advanced beyond the coalescence point on the ^{1}H NMR frequency range (400 MHz); we could, thus, detect the species present at high temperature and compare some of its spectral features to those of the species dominant at low temperature. For example, the ^{1}H NMR signal for the H3 proton in **4** moved from 3.22 ppm at −40 °C to 4.46 ppm at 90 °C, while the signals for the methylene tether (IndC*H*$_2$py) moved from ca. 3.80 to 2.70 ppm. Most of the other signals also moved with the temperature, but these were partially or completely overlapped by other signals. Unfortunately, the high-temperature ^{31}P{^{1}H} and ^{13}C{^{1}H} NMR spectra of **1** did not show any signals and thus did not contribute to a reliable identification of the complex formed at the high-temperature regime.

We propose that the dynamic process observed for complexes **1** and **2** can be adequately described by the equilibria depicted in Scheme 2. According to this proposal, the amino tether can coordinate to the Ni center to form the 18-electron intermediate (or transition state) shown; the equilibrium is driven further forward at higher temperatures and with the more nucleophilic amine moiety (CH$_2$Py > CH$_2$CH$_2$N(C$_4$H$_8$) ≈ CH$_2$CH$_2$NMe$_2$). This chelation step serves as model for the initial step of the ligand substitution reaction for the complexes IndNi(PR$_3$)Cl, which has been shown to proceed by an associative process.[11] The N→Ni coordination might be facilitated by either the slippage of the Ind ligand or the heterolytic dissociation of the Ni−Cl bond, which would form the chelating cations. Although the ionization of the Ni−Cl bond seemed

(11) Fontaine, F.; Dubois, M.-A.; Zargarian, D. *Organometallics* **2001**, *20*, 5145.

unlikely on the basis of our earlier work,[12] we were prompted to see if it would occur more readily in polar media.[13] Examination of the NMR spectra of **1** and **4** in DMSO and acetone showed that the ionization does take place quite readily; on the other hand, the spectra of samples in acetonitrile or chloroform resemble those of samples in toluene. It appears, therefore, that the dissociated Cl^- is not sufficiently solvated in the latter media and tends to return to the coordination sphere of Ni; thus, the full ionization is difficult to attain. Therefore, the available data point to the presence of an equilibrium process leading up to the cations, as shown in Scheme 2.

Ligand Exchange Reactions of the Cationic Complexes. The previous section described the results of NMR studies aimed at evaluating the extent of Ni−N interaction in the neutral complexes under study. We have carried out a series of ligand substitution reactions on the cationic complexes **4** and **5** in order to measure the relative strength of the N→Ni binding. Comparing the results of these studies to those of the analogous studies carried out on $[(\eta^3{:}\eta^1\text{-IndCH}_2\text{CH}_2\text{NMe}_2)\text{Ni}(\text{PPh}_3)]^+$ has shown that the pyridine moiety in **4** binds more strongly to Ni than do the NMe_2 and the pyrrolidine moieties, as described below.

Reacting 1 equiv of dppe with **4** or **5** resulted in the displacement of both PPh_3 and the chelating amine. The resulting complexes $[(\eta^3{:}\eta^0\text{-IndCH}_2\text{Py})\text{Ni}(\text{dppe})]^+$ (**9**) and $[\{\eta^3{:}\eta^0\text{-Ind}(\text{CH}_2)_2\text{N}(\text{C}_4\text{H}_8\}\text{Ni}(\text{dppe})]^+$ (**10**) were identified on the basis of their characteristic $^{31}P\{^1H\}$ NMR spectra, which displayed two broad signals due to the inequivalent P nuclei in these complexes (67.7 and 70.8 ppm for **9**, 68.4 and 65.3 ppm for **10**). The broadness of these signals is attributed to the hindered rotation of the Ind ligand; a similar observation has been made for the complex $[\{\eta^3{:}\eta^0\text{-Ind}(\text{CH}_2)_2\text{NMe}_2\}\text{Ni}(\text{dppe})]^+$, which was found to have a rotational energy barrier of 14.3 kcal mol^{-1}.[4a]

In contrast to their similar reactivities with dppe, complexes **4** and **5** reacted differently with PPh_3 and pyridine. Thus, reaction of **5** with PPh_3 led to an equilibrium between **5** and $[\{\eta^3{:}\eta^0\text{-Ind}(\text{CH}_2)_2\text{N}(\text{C}_4\text{H}_8)\}\text{Ni}(\text{PPh}_3)_2]^+$ (**8**); as before, the bis(phosphine) species was identified readily on the basis of its characteristic AB pattern in the $^{31}P\{^1H\}$ NMR spectrum ($CDCl_3$; 36.1 ppm (d, $^2J_{P-P} = 26.8$ Hz) and 31.9 (d, $^2J_{P-P} = 26.8$ Hz)). The k_{eq} was found to be 4.2 (±0.4), which is larger than the corresponding value of 0.9 for the equilibrium arising from the reaction of PPh_3 with $[\{\eta^3{:}\eta^1\text{-Ind}(\text{CH}_2)_2\text{NMe}_2\}\text{Ni}(\text{PPh}_3)]^+$.[4a] Similarly, the reaction of **5** with pyridine formed $[\{\eta^3{:}\eta^0\text{-Ind}(\text{CH}_2)_2\text{N}(\text{C}_4\text{H}_8)\}\text{Ni}(\text{PPh}_3)(\text{Py})]^+$ (**11**), which showed a new signal at 32.1 ppm in the $^{31}P\{^1H\}$ NMR spectrum; the k_{eq} in this case was 33 (±4), which is again larger than the corresponding value of 9 (±1) for the reaction of $[\{\eta^3{:}\eta^1\text{-Ind}(\text{CH}_2)_2\text{NMe}_2\}\text{Ni}(\text{PPh}_3)]^+$ with pyridine.[4a] We conclude, therefore, that the Ni−N bond is more labile in **5** relative to the NMe_2 analogue.

Contrary to the above reactivities, the reaction of complex **4** with excess PPh_3 (up to 45 equiv) resulted in the broadening of the original $^{31}P\{^1H\}$ NMR signal, but did not lead to the formation of the anticipated bis(PPh_3) cation. The reaction with pyridine also resulted in the broadening of the signal due to the coordinated PPh_3; in this case, however, the presence of >20 equiv of pyridine led to the disappearance of the signal for coordinated PPh_3 and the appearance of the signal for free PPh_3. Thus, excess PPh_3 does not displace the pyridine moiety, whereas excess pyridine displaces the coordinated PPh_3. It is significant that the presence of a chelating amine moiety should render the coordinated PPh_3 susceptible to displacement by an incoming amine ligand.[14]

Scheme 3

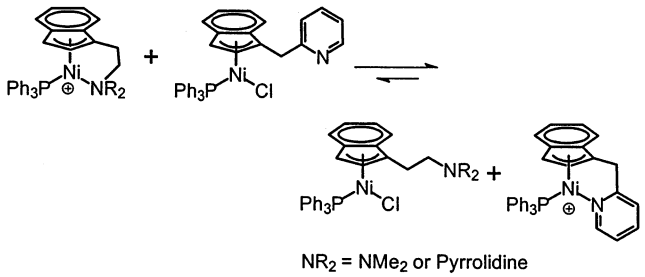

NR_2 = NMe_2 or Pyrrolidine

Taken together, the above results suggest that the strength of the Ni−N bond in these complexes follows the order **6** < **5** < $[(\eta^3{:}\eta^1\text{-Ind}(\text{CH}_2)_2\text{NMe}_2)\text{Ni}(\text{PPh}_3)]^+$ < **4**. This order is further supported by the observation that the neutral complex **1** reacts with the cations **5** or $[(\eta^3{:}\eta^1\text{-Ind}(\text{CH}_2)_2\text{NMe}_2)\text{Ni}(\text{PPh}_3)]^+$ to form **4** and the corresponding neutral complex $(\text{IndCH}_2\text{CH}_2\text{NR}_2)\text{Ni}(\text{PPh}_3)\text{Cl}$ ($R_2 = Me_2$ or $(CH_2)_4$) (Scheme 3).

Electrochemical Studies. It is reasonable to assume that, all other factors being equal, the electron density of the Ni center in the complexes $(\text{Ind}\wedge\text{NR}_2)\text{Ni}(\text{PPh}_3)\text{Cl}$ and $[(\eta^3{:}\eta^1\text{-Ind}\wedge\text{NR}_2)\text{Ni}(\text{PPh}_3)]^+$ should reflect the degree of the N→Ni interaction, stronger interactions leading to more electron-rich Ni centers. Thus, in principle, a direct correlation should exist between the strength of the Ni−N bond, as determined from NMR studies described in the preceding two sections, and the electron density at Ni, as inferred from the reduction potential of the complex. To determine the effect of N→Ni binding on the electron density at the Ni center, we have used cyclic voltammetry to measure the reduction potentials of complexes **1**−**5**, $(\text{IndCH}_2\text{CH}_2\text{NMe}_2)\text{Ni}(\text{PPh}_3)\text{Cl}$, and $[(\eta^3{:}\eta^1\text{-Ind}(\text{CH}_2)_2\text{NMe}_2)\text{Ni}(\text{PPh}_3)]^+[\text{BPh}_4]^-$. The electrochemical measurements showed that these complexes undergo irreversible, one-electron reduction. The reduction potentials of these compounds and those of related complexes not having any Ni−N interaction were measured and corrected against the standard calomel electrode (SCE) and are listed in Table 3. These data allow the following observations:[15]

(a) The cationic species are easier to reduce than the neutral ones, as anticipated.

(12) For instance, analogous Ni−Cl complexes bearing nonfunctionalized Ind substituents do not undergo ionization even in the presence of very strongly donating ligands such as phosphines.

(13) We would like to thank one of the reviewers of our manuscript for suggesting that we reexamine this issue.

(14) The generally stronger binding of phosphines vs amines to low-valent late transition metals is well documented: (a) Collman, J. P.; Hegedus, L. S.; Norton, J. R.; Finke, R. G. *Principles and Applications of Organotransition Metal Chemistry*; University Science Books: Mill Valley, CA, 1987; p 241, and references therein. (b) Li, M. P.; Drago, R. S.; Pribula, A. J. *J. Am. Chem. Soc.* **1977**, *99*, 6900. (c) de Graaf, W.; Boersma, J.; Smeets, W. J. J.; Spek, A. L.; van Koten, G. *Organometallics* **1989**, *8*, 2907. (d) Wang, L.; Wang, C.; Bau, R.; Flood, T. C. *Organometallics* **1996**, *15*, 491. (e) Widenhoefer, R. A.; Buchwald, S. L. *Organometallics* **1996** *15*, 2755. (f) Widenhoefer, R. A.; Buchwald, S. L. *Organometallics* **1996**, *15*, 3534. (g) Pfeiffer, J.; Kickelbick, G.; Schubert, U. *Organometallics* **2000**, *19*, 62.

(b) For both the neutral and cationic complexes, the derivatives bearing the NMe_2 moiety were more difficult to reduce. For instance, the complexes **1**−**3** are reduced at −1.36 to −1.34 V, compared to −1.41 V for (IndCH$_2$CH$_2$NMe$_2$)Ni(PPh$_3$)Cl; the cations **4** (−1.05 V) and **5** (−1.08 V) were also easier to reduce than [(η^3:η^1-Ind(CH$_2$)$_2$NMe$_2$)Ni(PPh$_3$)]$^+$ (−1.16 V). Clearly, the nature of the tethered amine moiety modulates the level of electron density at the Ni center.

(c) The relatively easier reduction of the complexes not possessing a chelating moiety (e.g., (1-Me-Ind)Ni(PPh$_3$)Cl: E_{Red} = −1.26 V) shows that the N→Ni interaction causes a net increase in the electron density at the Ni center in the neutral species. On the other hand, replacing the chelating amine donor in the cationic complexes by a second PPh_3 ligand results in a greater net transfer of electron density to Ni in the cationic species (e.g., [(1-Me-Ind)Ni(PPh$_3$)$_2$]$^+$: E_{Red} = −1.24 V).

According to the data listed in Table 3, the electron density at the Ni center decreases in the order (IndCH$_2$CH$_2$NMe$_2$)Ni(PPh$_3$)Cl > **1** ≈ **2** ≈ **3** and [(IndCH$_2$CH$_2$NMe$_2$)Ni(PPh$_3$)]$^+$ > **5** > **4**. On the other hand, the NMR studies indicated the following relative orders of N→Ni interactions: **1** > (IndCH$_2$CH$_2$NMe$_2$)Ni(PPh$_3$)Cl ≈ **2** > **3** and **4** > [(η^3: η^1-IndCH$_2$CH$_2$NMe$_2$)Ni(PPh$_3$)]$^+$ > **5**. Comparison of these orders reveals that the complexes bearing the pyridine moiety (i.e., **1** and **4**) seem to defy the predicted correlation between Ni−N bond strength and the reduction potential. This anomaly might be rationalized in terms of the π-acidity of the pyridine moiety: Ni→N π-back-bonding would be expected to reinforce the Ni−N interaction in **1** and **4**, which would be reflected in the NMR spectra, but it would also reduce the net electron density of the Ni center, which would be reflected in the reduction potentials of these complexes. The existence of some degree of Ni→N π-back-bonding is also evident from the structural parameters of complex **4**. For example, the Ni−N bond is somewhat shorter and the Ni−Ind interaction is somewhat stronger in **4** than in [(η^3: η^1−IndCH$_2$CH$_2$NMe$_2$)Ni(PPh$_3$)]$^+$ (Ni−N = 1.95 vs 2.01 Å, Δ(M−C) = 0.24 vs 0.26 Å).

In conclusion, the electrochemical measurements are very sensitive to the net electrophilicity of the Ni center in these complexes, whereas the NMR studies can evaluate the relative lability of the Ni−N chelation. There exists some correlation between these parameters, except in cases where there is Ni→N π-back-bonding. While it might seem counterintuitive to suggest that the cationic Ni center is engaged in significant back-bonding to the pyridine moiety, the above data support this possibility.

(15) One of the reviewers of our manuscript has asked for a justification for the use of reduction potentials in this context in light of the irreversibility of the reduction process. Strictly speaking, the reduction potential of an irreversible reduction (or oxidation) process might vary as a function of many different parameters such as electrolyte composition and nature of electrode. It is common practice, however, to consider that in situations where an analogous series of compounds are being studied under identical conditions the values of reduction potential can be related, to a good approximation, to structural or electronic properties of the compounds. In the present case, since we are dealing with a family of complexes possessing very similar structural features and compositions, and since the electrochemical studies were performed under identical conditions, we believe that the reduction potential values represent fairly accurately the electron richness of the metal centers in this family of complexes.

Polymerization of Olefins. Many cationic Ni complexes are active in the catalytic polymerization and oligomerization of olefins.[16] We have reported recently that systems consisting of IndNi(PR$_3$)X and methylaluminoxane (MAO) catalyze both the dimerization and polymerization of ethylene;[17] on the other hand, the dimerization of ethylene (but not its polymerization) is also promoted by the highly electrophilic cations generated in-situ from the complexes (Ind)Ni(PR$_3$)(OTf).[18] The available mechanistic information indicates that the dimerization of ethylene in these systems proceeds by an initial insertion of ethylene into the Ni−Ind bond; subsequent β-H elimination from the resulting alkyl ligand releases CH$_2$=CH−Ind (detected in some cases[18]) and generates a postulated, cationic, Ind-free Ni−H species that serves as the main catalyst. The mechanistic details of the ethylene polymerization reaction are not known with certainty, but the involvement of cationic species such as [IndNi(PR$_3$)]$^+$ in these reactions has been ruled out.[17]

Subsequent studies showed that cations bearing chelating amine moieties such as [(η^3:η^1-Ind(CH$_2$)$_2$NMe$_2$)Ni(PPh$_3$)]$^+$ are also active in the dimerization of ethylene (in the presence of MAO)[4b] and the polymerization of styrene (without cocatalysts).[4a] Although the dimerization of ethylene by these systems might operate by the insertion-type mechanisms discussed above, the polymerization of styrene can also proceed via carbocationic[19] or radical[20] pathways. It should be noted, however, that the complex [(η^3:η^1-Ind(CH$_2$)$_2$NMe$_2$)Ni(PPh$_3$)]$^+$ does not promote the polymerization of other monomers such as ethyl(vinyl) ether or methyl methacrylate, which are very prone to carbocationic[21] or radical[22] polymerizations, respectively.

As a follow-up to the latter studies, we have examined the polymerization activities of the cationic complexes **4**−**6** in order to assess the influence of the tether on these reactions. The bulk of our studies has concentrated on the polymerization of styrene, because it gave the most informative results among the monomers tested (e.g., norbornene gave <5% yields of an in-

(16) (a) Johnson, L. K.; Killian, C. M.; Arthur, S. D.; Feldman, J.; McCord, E. F.; McLain, S. J.; Kreutzer, K. A.; Bennett, M. A.; Coughlin, E. B.; Ittel, S. D.; Parthasarathy, A.; Tempel, D. J.; Brookhart, M. S. DuPont, WO 96/23010, 1996. (b) Johnson, L. K.; Killian, C. M.; Brookhart, M. S. *J. Am. Chem. Soc.* **1995**, *117*, 6414. (c) Keim, W.; Appel, R.; Gruppe, S.; Knoch, F. *Angew. Chem.* **1987**, *99*, 1042. (d) Ostoja-Starzewski, K. A.; Witte, J. *Angew. Chem.* **1985**, *97*, 610. (e) Flid, V. R.; Kuznetsov, V. B.; Grigor'ev, A. A.; Belov, A. P. *Kinetics Catal.* **2000**, *41*(5), 604. (f) Flid, V. R.; Manulik, O. S.; Grigor'ev, A. A.; Belov, A. P. *Kinetics Catal.* **2000**, *41*(5), 658. (g) Goodall, B. L.; Benedikt, G. M.; McIntosh, L. H.; Barnes, D. A. U.S. Patent-5468819, 1995. (h) Goodall, B. L.; Benedikt, G. M.; McIntosh, L. H.; Barnes, D. A.; Rhodes, L. F. U.S. Patent-5468819, 1995. (i) Bonnet, M. C.; Dahan, F.; Ecke, A.; Keim, W.; Schulz, R. P.; Tkatchenko, I. *J. Chem. Soc., Chem. Commun.* **1994**, 615. (j) Aresta, M.; Dibenedetto, A.; Quaranta, E.; Lanfanchi, M.; Tiripicchio, A. *Organometallics* **2000**, *19*, 4199. (k) Ihara, E.; Fujimura, T.; Yasuda, H.; Maruo, T.; Kanehisa, N.; Kai, Y. *J. Polym. Sci.*: *Part A*: *Polym. Chem.* **2000**, *38*, 4764.

(17) Dubois, M.-A.; Wang, R.; Zargarian, D.; Tian, J.; Vollmerhaus, R.; Li, Z.; Collins, S. *Organometallics* **2001**, *20*, 663.

(18) Wang, R.; Groux, L. F.; Zargarian, D. *Organometallics* **2002**, *21*, 5531.

(19) (a) Yang, M.-L.; Li, K.; Stöver, H. H. *Macromol. Rapid Commun.* **1994**, *15*, 425. (b) Satoh, K.; Nakashima, J.; Kamigaito, M.; Sawamoto, M. *Macromolecules* **2001**, *34*, 396.

(20) (a) Li, P.; Qiu, K.-Y. *Polymer* **2002**, *43*, 5873. (b) Grognec, E. L.; Claverie, J.; Poli, R. *J. Am. Chem. Soc.* **2001**, *123*, 9513.

(21) (a) Wang, Q.; Baird, M. C. *Macromolecules* **1995**, *28*, 8021. (b) Baird, M. C. *Chem. Rev.* **2000**, *100*, 1471.

(22) Xia, J.; Matyjaszewski, K. *Macromolecules* **1997**, *30*, 7692, and references therein.

Table 4. Polymerization of Styrene Catalyzed by Complexes 4, 5, and 6[a]

					high M_w polymers		low M_w oligomers	
run	cat.	T (°C)	time (h)	TON	M_w ($\times 10^3$)	M_w/M_n	M_w ($\times 10^3$)	M_w/M_n
1	**4** or **5**	20	48	0				
2	**4**	40	48	127			1.9	5.7
3	**4**	60	48	207	134	1.4	3.0	1.5
4	**4**	80	48	554	200	1.3		
5	**5**	40	48	35			2.3	1.2
6	**5**	60	48	180	153	1.6	3.0	1.4
7	**5**	80	48	486	145	1.7		
8	**6**[a]	80	48	1519	22.9	3.0		
9a	**4**	60	1	47			1.8	1.0
9b			4.5	86			3.8	1.5
9c			7	142			4.0	1.5
9d			24	163	184	1.4	4.4	1.6
9e			30	185	191	1.2	4.2	1.6
9f			48	207	193	1.3	4.3	1.6

[a] Prepared in-situ by combining **3** with 5 equiv of $NaBPh_4$.

tractable material). We have also studied briefly the reactivity of *N*-vinylcarbazole, which is prone to carbocationic[23] or radical[24] polymerizations, to address the mechanistic issues alluded to above. To compare the results of the present studies with those obtained from our previous studies with the $(CH_2)_2NMe_2$ analogue, we have performed most of the polymerization experiments under similar conditions, i.e., stirring the appropriate precatalyst and 1000−2000 equiv of monomer in CH_2Cl_2 or dichloroethane at 20−80 °C over 48 h. In experiments involving complex **6**, given the above-mentioned difficulty in isolating pure samples of this complex, we have used a combination of **3**/$NaBPh_4$ (1:5) to generate this species in-situ.

Initial tests showed that the reaction temperature had a very important influence on the course of the polymerization reaction, giving different results in terms of catalytic turnover numbers (TON), M_w of the products, and polydispersity index values (M_w/M_n). Thus, neither **4** nor **5** reacted with the monomers at room temperature (run 1, Table 4), presumably because the relatively strong Ni−N bond does not break to facilitate the coordination of the monomer. On the other hand, the reaction of **4** with styrene at 40 °C resulted in low M_w oligomers (run 2); increasing the temperature to 60 °C gave a bimodal distribution of high M_w polymers and low M_w oligomers (run 3), whereas at 80 °C we obtained a fairly narrow distribution of high M_w species (run 4). Higher temperatures also led to higher activities (i.e., larger TON values). Similar observations were made for the polymeriztion of styrene catalyzed by **5** (runs 5−7).

In contrast to the reactivities of **4** and **5**, the polymerization of styrene in the presence of in-situ-generated **6** did proceed at room temperature, albeit with low yields and smaller M_w. Moreover, polymerization of styrene catalyzed by **6** at higher temperatures also gave much higher yields compared to the corresponding polymerizations catalyzed by **4** or **5**; on the other hand, the poly(styrene) obtained from the reaction of **6** displayed a unimodal distribution of fairly low M_w species (run 8).

The above results demonstrate that, among the complexes studied, in-situ-generated **6** is the most active precatalyst for the polymerization of styrene, which is consistent with the weak Ni−N interaction in this complex. The precatalysts **4** and **5** possess similar activities, although **4** appears to give somewhat higher TON values. On the other hand, all of these precatalysts are more active than $[(\eta^3{:}\eta^1\text{-Ind}(CH_2)_2NMe_2)Ni(PPh_3)]^+$. On a first approximation, this order of reactivity seems to correlate with the electrochemical properties of these cationic complexes (Table 3): the most Lewis acidic cation (i.e., the one easiest to reduce) appears to be the most active catalyst for the polymerization of styrene. Thus, the nature of the amine moiety in Ind∧NR_2 ligands modulates both the electrophilicity of the Ni center and its polymerization activity.

The importance of the nature of the tethered amine moiety on the reactivity of the complexes indicates that the Ind ligand remains coordinated to the Ni center, which implies, in turn, that the insertion-type mechanism described above for the dimerization of ethylene is not likely to be the polymerization pathway for styrene. To test the feasibility of a carbocationic propagation, we examined the reaction of *N*-vinylcarbazole; the reactions were carried out in the dark in order to avoid light-induced radical polymerization. This monomer does indeed react with complex **4** (1:100 ratio; 80 °C) to give a solid (95% yield) consisting of a broad mixture of oligomers (GPC in THF: M_w between 23 725 and 367, maximum at 575); the reaction with **5** under the same conditions gave a solid with shorter oligomers (M_w between 2760 and 360, maximum at 433). For comparison, polymerization of this electron-rich olefin by the cationic complex $[L_2Pt(Me)(MeCN)]^+$ (L_2 = diaryldiazabutadienes) gives polymers with M_w values of ca. 23 000 and M_w/M_n of ca. 3 (at room temperature),[23a] while initiation with the Lewis acid $B(C_6F_5)_3$ gives polymers with M_w values of ca. 100 000 and M_w/M_n of ca. 3.6 (at −78 °C).[21a]

The above results seem to favor a carbocationic pathway for the polymerization of styrene and *N*-vinylcarbazole by the complexes **4**/**5**. To gain further insight on the course of the styrene polymerization reaction in these systems, we monitored the progress of a typical polymerization experiment (reaction of **4** with styrene at 60 °C, run 9) by performing GPC analyses on 1 mL samples of the reaction mixture after 1, 4.5, 7, 24, 30, and 48 h. The results of this experiment show that the reaction generated mainly oligomers (up to M_w of ca. 4000) during the initial stages. A steady increase was noted in M_w values as a function of time such that after a few hours the system seems to convert the oligomers into high M_w polymers, which constitute the dominant products after ca. 24 h. This reaction profile can be interpreted as implying that the polymerization reactions promoted by **4** proceed via two distinct pathways, one that is active throughout the experiment and generates oligomers and another that is activated after a few hours and generates longer chain polymers.

To delineate the importance of continued heating for the polymerization process, two reactions were carried out under standard conditions (**4**/styrene/dichloroethane/80 °C/48 h) with the difference that one was

(23) (a) Albietz, P. J.; Kaiyuan, Y.; Eisenberg, R. *Organometallics* **1999**, *18*, 2747. (b) Cho, H.-N.; Choi, S.-K. *J. Polym. Sci. A: Polym. Chem.* **1987**, *25*, 1769, and references 5−10 therein. (c) Bowyer, P. M.; Ledwith, A.; Sherrington, D. C. *Polymer* **1971**, *12*, 509.

(24) (a) Ellinger, L. P. *Polymer* **1964**, *5*, 559. (b) Jones, R. G.; Khalid, N. *Makrom. Chem.* **1982**, *26*, 625.

heated only during the initial 2 h of the polymerization reaction, while the other was heated throughout the entire experiment. Analysis of the polymers showed that the partially heated reaction gave about a quarter of the yield of the poly(styrene) obtained from the other, indicating that higher temperatures are necessary not only for initiating the polymerization reaction but also for sustaining it.

Another experiment was carried out in order to answer the important question of whether PPh_3 remains coordinated to Ni during the polymerization reaction. Thus, we followed a polymerization experiment by monitoring the ^{31}P NMR spectrum of a 0.016 M solution of complex **4** containing 100 equiv of styrene (0.5 mL $ClCH_2CH_2Cl$/0.1 mL C_6D_6) at 50 °C. The NMR spectra did not show the presence of a free phosphine, implying that this ligand remains coordinated to Ni during the reaction; by inference, we believe that it is the amine moiety that detaches from the Ni center to open up a coordination site. As mentioned above, the displacement of the chelating amine ligand is slow at low temperatures, and so initiation of the catalysis requires higher temperatures. It is not clear, however, why the high temperatures must be sustained throughout the polymerization, because carbocationic propagation should not require high temperatures.[21b]

Conclusion

The preparation of the neutral and cationic complexes **1**−**6** has allowed us to study in more detail the effect of placing a hemilabile amino moiety adjacent to the Ni center in this family of complexes. Studying the reversible coordination of the amine moiety in the neutral complexes and measuring the impact of N→Ni coordination on the reduction potentials of these complexes have allowed us to gauge the nucleophilicity of the hemilabile moiety. The correlation between the electrophilicity of the Ni center in the cationic complexes and their catalytic activities provides a convenient means of predicting catalytic activity on the basis of simple ligand kinetics and electrochemical measurements. Although our results do not provide strong support for the involvement of a carbocationic pathway in the polymerization reactions, this possibility is most consistent with the experimental observations.

Experimental Section

General Comments. All manipulations except the GPC analyses were performed under an inert atmosphere of N_2 using standard Schlenk techniques and a drybox. Dry, oxygen-free solvents were prepared by distillation from appropriate drying agents and employed throughout. The substituted indenyl ligands have been prepared by adding the appropriate Cl∧NR_2 to a solution of LiInd, as described previously.[5] All other reagents used in the experiments were obtained from commercial sources and used as received. The elemental analyses were performed by the Laboratoire d'Analyse Élémentaire (Université de Montréal). The spectrometers used for recording the NMR spectra are Bruker AMXR400 (^1H (400 MHz), $^{13}C\{^1H\}$ (100.56 MHz), and $^{31}P\{^1H\}$ (161.92 MHz)) and Bruker AV300 (^1H (300 MHz) and $^{31}P\{^1H\}$ (121.49 MHz)). $^{13}C\{^1H\}$-CP-MAS (75.49 MHz) spectra were recorded on a Bruker DSX300 spectrometer.

Crystal Structure Determinations. Dark red crystals of **1** were obtained from a −20 °C Et_2O solution of **1**. The crystal data for **1** were collected on a Nonius CAD-4 diffractometer with graphite-monochromated Cu Kα radiation at 293(2) K using CAD-4 software. The refinement of the cell parameters was done with the CAD-4 software,[25] and the data reduction used NRC-2 and NRC-2A.[26] Dark red crystals of **4** were obtained from a −20 °C CH_2Cl_2/Et_2O solution of **4**. The crystal data for **4** were collected on a Bruker AXS SMART 2K diffractometer with graphite-monochromated Cu Kα radiation at 223(2) K using SMART.[27] Cell refinement and data reduction were done using SAINT.[28] Both structures were solved by direct methods using SHELXS97[29] and difmap synthesis using SHELXL96;[30] the refinements were done on F^2 by full-matrix least squares. All non-hydrogen atoms were refined anisotropically, while the hydrogens (isotropic) were constrained to the parent atom using a riding model. Crystal data and experimental details for **1** and **4** are listed in Table 1, and selected bond distances and angles are listed in Table 2.

(η^3:η^0-IndCH$_2$Py)Ni(PPh$_3$)Cl (1). An Et_2O solution (250 mL) containing $IndCH_2Py$ (300 mg, 1.45 mmol) and BuLi (0.58 mL of a 2.5 M solution in hexane) was stirred for 4 h at room temperature and then transferred (dropwise over 1.5 h) to a stirred slurry of $(PPh_3)_2NiCl_2$ (1.23 g, 1.89 mmol) in Et_2O (50 mL). The dark red solution was then filtered, and the solvent volume was reduced to ca. 75 mL. A dark red powder precipitated as fairly pure product (160 mg, 0.28 mmol, 20% yield), which was recrystallized from cold Et_2O to give crystals suitable for X-ray analysis. $^{31}P\{^1H\}$ NMR (toluene-d_8, −40 °C): 30.6 ppm. ^1H NMR (toluene-d_8, −40 °C): 7.50 and 7.00 (m, py and PPh_3), 7.33 (m, H7), 7.24 (m, H6), 6.60 (m, H5), 6.43 (H2), 6.05 (d, $^3J_{H-H}$ = 7.6 Hz, H4), 3.80 and 3.66 (m, Ind-CH_2), 3.22 (H3). $^{13}C\{^1H\}$ CP-MAS: 157.9 (C9), 152.1 (C13), 134.9 (C11), 133.3 (*o*-C PPh_3), 130.0, 129.4 and 128.1 (C10/*p*-C and *m*-C PPh_3), 126.9 and 125.7 (C5/C6)), 121.6 and 120.7 (C7/C12), 115.9 (C4), 107.3 (C1), 104.3 (C2), 68.1 (C3), 35.7 (IndCH_2). Anal. Calcd for $C_{33}H_{27}PNiNCl$: C, 70.44; H, 4.84; N, 2.49. Found: C, 70.56; H, 4.91; N, 2.11.

{η^3:η^0-Ind(CH$_2$)$_2$N(C$_4$H$_8$)}Ni(PPh$_3$)Cl (2). An Et_2O solution (200 mL) containing $Ind(CH_2)_2NC_4H_8$ (1.00 g, 4.69 mmol) and BuLi (1.88 mL of a 2.5 M solution in hexane) was stirred for 5 h and then transferred (dropwise over 2 h) to a stirred slurry of $(PPh_3)_2NiCl_2$ (3.7 g, 5.6 mmol) in Et_2O (30 mL). Half of the solvent was then evaporated and the solution filtered. The filtrate volume was further reduced to ca. 50 mL and the resulting solution cooled to −15 °C. A first crop of the desired product (ca. 1 g of a reddish solid) was isolated. Recrystallization from CH_2Cl_2/pentane gave 550 mg of pure product (0.97 mmol, 21% yield). $^{31}P\{^1H\}$ NMR ($CDCl_3$): 30.7 ppm. ^1H NMR ($CDCl_3$, −40 °C): 7.7−7.0 (PPh_3, H6 and H7), 6.96 (H5), 6.60 (H2), 6.04 (H4), 3.50 (H3) 3.06 and 2.87 (CH_2N), 2.62 (NCH_2 cycle), 2.18 (IndCH_2), 1.82 (NCH$_2$CH_2 cycle). $^{13}C\{^1H\}$ NMR ($CDCl_3$, −40 °C): 133.9 (d, $^2J_{P-C}$ = 11 Hz, *o*-C of PPh_3), 132.1 and 131.9 (C3A/C7A), 131.1 (d, $^1J_{P-C}$ = 44.8 Hz, *i*-C of PPh_3), 130.4 (*p*-C of PPh_3), 128.3 (d, $^3J_{P-C}$ = 9 Hz, *m*-C of PPh_3), 126.7 and 126.3 (C5/C6), 117.9 and 116.4 (C4/C7), 104.9 (d, $^2J_{P-C}$ = 14 Hz, C1), 103.0 (C2), 67.1 (C3), 54.1 (NCH_2, cycle), 53.1 (CH_2N), 26.2 (IndCH_2), 23.2 (NCH$_2$CH_2, cycle). Anal. Calcd for $C_{33}H_{33}PNiNCl$: C, 69.69; H, 5.85; N, 2.46. Found: C, 69.33; H, 5.83; N, 2.44.

{η^3:η^0-Ind(CH$_2$)$_2$N(*i*-Pr)$_2$}Ni(PPh$_3$)Cl (3). An Et_2O solution (200 mL) containing $Ind(CH_2)_2N(i\text{-}Pr)_2$ (800 mg, 3.29

(25) *CAD-4 Software*, Version 5.0; Enraf-Nonius: Delft, The Netherlands, 1989.
(26) Gabe, E. J.; Le Page, Y.; Charlant, J.-P.; Lee, F. L.; White, P. S. *J. Appl. Crystallogr.* **1989**, *22*, 384.
(27) *SMART*, Release 5.059; Bruker Molecular Analysis Research Tool; Bruker AXS Inc.: Madison, WI 53719-1173, 1999.
(28) *SAINT*, Release 6.06; Integration Software for Single-Crystal Data; Bruker AXS Inc.: Madison, WI 53719-1173, 1999.
(29) Sheldrick, G. M. *SHELXS*, Program for the Solution of Crystal Structures; University of Goettingen: Germany, 1997.
(30) Sheldrick, G. M. *SHELXL*, Program for the Refinement of Crystal Structures; University of Goettingen: Germany, 1996.

mmol) and BuLi (1.31 mL of a 2.5 M solution in hexane) was stirred for 16 h at room temperature and then transferred (dropwise over 2 h) to a stirred slurry of $(PPh_3)_2NiCl_2$ (2.8 g, 4.3 mmol) in Et_2O (50 mL). The mixture was then filtered, and the filtrate volume was reduced to ca. 20 mL and cooled to −15 °C. The pure product was isolated as a dark red powder after multiple precipitation from cold ether and washings with hot hexanes (630 mg, 1.05 mmol, 32% yield). $^{31}P\{^1H\}$ NMR (C_6D_6): 30.8 ppm. ^1H NMR (C_6D_6): 7.66 and 6.98 (PPh_3), 7.30 (d, $^3J_{H-H}$ = 7.8 Hz, H7), 7.10 (t, $^3J_{H-H}$ = 7.8 Hz, H6), 6.83 (t, $^3J_{H-H}$ = 7.6 Hz, H5), 6.60 (H2), 6.10 (d, $^3J_{H-H}$ = 7.6 Hz, H4), 3.43 (H3), 3.05 and 2.98 (m, Ind-CH_2CH_2N), 2.40 and 2.26 (NCHMe$_2$), 1.01 (m, NCH(CH_3)$_2$). $^{13}C\{^1H\}$ NMR (C_6D_6): 134.6 (d, $^2J_{P-C}$ = 11 Hz, *o*-C of PPh_3), 132.8 (d, $^1J_{P-C}$ = 42.8 Hz, *i*-C of PPh_3), 130.3 (*p*-C of PPh_3), 128.5 (*m*-C of PPh_3), 126.5 and 126.2 (C5/C6), 118.7 and 116.9 (C4/C7), 106.8 (C1), 103.7 (C2), 66.9 (C3), 48.4 (NCHMe$_2$), 42.4 (CH$_2$N), 29.0 (Ind$C$H$_2$), 21.1 (NCH(CH$_3$)$_2$). Anal. Calcd for $C_{35}H_{39}PNiClN$: C, 70.20; H, 6.56; N, 2.34. Found: C, 69.84; H, 6.81; N, 2.18.

[(η^3:η^1-IndCH$_2$Py)Ni(PPh$_3$)][BPh$_4$] (4). A CH_2Cl_2 solution (10 mL) containing (IndCH$_2$Py)Ni(PPh_3)Cl (200 mg, 0.36 mmol) and $NaBPh_4$ (730 mg, 2.2 mmol) was stirred for 24 h and then filtered. The filtrate volume was reduced to ca. 1 mL, and Et_2O (ca. 20 mL) was added to precipitate the product. Repeated precipitation gave the pure product as an orange powder (175 mg, 0.21 mmol, 58% yield). $^{31}P\{^1H\}$ NMR ($CDCl_3$): 33.1 ppm; (CD_2Cl_2): 34.6 ppm. ^1H NMR (CD_2Cl_2): 7.6−6.7 (PPh_3, BPh_4, H5 to H7, py), 6.93 (d, $^3J_{H-H}$ = 5.5 Hz, H2), 6.52 (t, $^3J_{H-H}$ = 6.6 Hz, H5), 6.10 (d, $^3J_{H-H}$ = 7.7 Hz, H4), 4.06 (H3), 3.87 and 3.57 (d, $^2J_{H-H}$ = 18.1 Hz, IndCH_2). $^{13}C\{^1H\}$ NMR (CD_2Cl_2): 175.7 (d, $^2J_{P-C}$ = 7 Hz, C9), 163.8 (4-line multiplet, J_{B-C} = 49 Hz, *i*-C of BPH_4), 152.4 (d, $^2J_{P-C}$ = 4 Hz, C13), 139.1 (C11), 135.8 (*m*-C of BPH_4), 133.6 (d, $^2J_{P-C}$ = 12 Hz, *o*-C of PPh_2), 131.6 (*p*-C of PPh_2), 129.2 (d, $^3J_{P-C}$ = 10 Hz, *m*-C of PPh_2), 128.9, 128.6, and 128.5 (*i*-C of PPh_2/C5/C6), 125.5 (*o*-C of BPH_4), 124.7 (C10), 124.6 and 124.4 (C3A/C7A), 123.4 (C12), 121.6 (*p*-C of BPH_4), 118.3 and 117.9 (C4/C7), 108.7 (C2), 100.9 (d, $^2J_{P-C}$ = 8 Hz, C1), 72.3 (C3), 34.5 (IndCH_2). Anal. Calcd for $C_{57}H_{47}PNiNB$: C, 80.88; H, 5.60; N, 1.66. Found: C, 80.55; H, 5.86; N, 1.73.

[{η^3:η^1-Ind(CH$_2$)$_2$N(C$_4$H$_8$)}Ni(PPh$_3$)][BPh$_4$] (5). A CH_2Cl_2 solution (20 mL) containing {Ind(CH$_2$)$_2$N(C$_4$H$_8$)}Ni(PPh_3)Cl (300 mg, 0.53 mmol) and $NaBPh_4$ (1.08 g, 3.16 mmol) was stirred for 4 h and then filtered. The filtrate volume was reduced to ca. 6 mL, and Et_2O (ca. 30 mL) was added to precipitate the product. Repeated precipitation gave the pure product as an orange powder (280 mg, 62% yield). $^{31}P\{^1H\}$ NMR ($CDCl_3$): 30.3 ppm. ^1H NMR ($CDCl_3$): 7.6−6.9 (PPh_3, BPh_4, H5 to H7), 6.80 (H2), 5.50 (d, $^2J_{H-H}$ = 7.4 Hz, H4), 3.97 (H3), 2.55 (m, IndCH_2), 2.4 to 1.4 (m, NCH_2), 1.2 to 0.6 (NCH$_2$CH_2). $^{13}C\{^1H\}$ NMR ($CDCl_3$): 163.5 (4-line multiplet, J_{B-C} = 49 Hz, *i*-C of BPH_4), 136.5 (*m*-C of BPH_4), 133.7 (d, $^2J_{P-C}$ = 12 Hz, *o*-C of PPh_2), 131.7 (*p*-C of PPh_2), 129.3 (d, $^3J_{P-C}$ = 10 Hz, *m*-C of PPh_2), 129.3 (d, $^1J_{P-C}$ = 36 Hz, *i*-C of PPh_2), 128.4 and 127.7 (C5/C6), 126.9 and 123.9 (C3A/C7A), 125.7 (*o*-C of BPH_4), 121.9 (*p*-C of BPH_4), 118.4 and 118.3 (C4/C7), 109.8 (d, J_{P-C} = 10 Hz, C1), 106.8 (C2), 70.7 (C3), 70.1, 59.7 and 58.4 (CH$_2$N), 23.7 (IndCH_2), 21.3 and 21.1 (NCH$_2$CH_2). Anal. Calcd for $C_{57}H_{53}PNiNB$: C, 80.31; H, 6.27; N, 1.64. Found: C, 80.39; H, 6.54; N, 1.52.

Reaction of {Ind(CH$_2$)$_2$N(*i*-Pr)$_2$}Ni(PPh$_3$)Cl (3) with NaBPh$_4$. {Ind(CH$_2$)$_2$N(*i*-Pr)$_2$}Ni(PPh_3)Cl (31 mg, 0.05 mmol) and $NaBPh_4$ (106.3 mg, 0.31 mmol) were stirred in CH_2Cl_2 (80 mL) for 4 h, filtered, and evaporated. The resulting solid was dissolved in CH_2Cl_2 (0.75 mL) and precipitated by adding hexanes (40 mL). The $^{31}P\{^1H\}$ NMR ($CDCl_3$) spectrum showed four major signals, as follows: 29.3, attributed to [{η^3:η^1-Ind(CH$_2$)$_2$N(*i*-Pr)$_2$}Ni(PPh_3)][BPh_4] (**6**); 30.7, attributed to unreacted **3**; 32.1 and 36.5 (d, $^2J_{P-P}$ = 25 Hz), attributed to [{η^3:η^0-Ind(CH$_2$)$_2$N(*i*-Pr)$_2$}Ni(PPh_3)$_2$][BPh_4] (**7**).

Chart 1

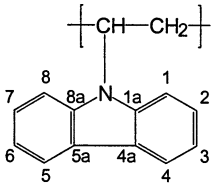

[{η^3:η^0-Ind(CH$_2$)$_2$N(*i*-Pr)$_2$}Ni(PPh$_3$)$_2$][BPh$_4$] (7). {Ind(CH$_2$)$_2$N(*i*-Pr)$_2$}Ni(PPh_3)Cl (95.4 mg, 0.16 mmol), PPh_3 (360 mg, 1.37 mmol), and $NaBPh_4$ (340 mg, 1.0 mmol) were stirred in CH_2Cl_2 (20 mL) for 4 h, then filtered and evaporated. The resulting solid was dissolved in CH_2Cl_2 (2 mL) and precipitated by adding hexanes (50 mL). Repeated recrystallizations did not give a pure product because the dissociation of one of the phosphines allowed the chelation of the tether to produce [{η^3:η^1-Ind(CH$_2$)$_2$N(*i*-Pr)$_2$}Ni(PPh_3)][BPh_4] (6−10%). $^{31}P\{^1H\}$ NMR ($CDCl_3$): 36.8 (d, $^2J_{P-P}$ = 25 Hz) and 32.5 (d, $^2J_{P-P}$ = 25 Hz). ^1H NMR ($CDCl_3$): 7.6−6.9 (PPh_3, BPh_4, H5 to H7), 6.51 (H2), 6.25 (d, $^2J_{H-H}$ = 6.5 Hz, H4 or H7), 6.02 (d, $^2J_{H-H}$ = 7.4 Hz, H4 or H7), 4.89 (d, $^2J_{H-H}$ = 3.2 Hz, H3), 2.75 (m, NCH_2), 2.35 and 2.28 (m, IndCH_2), 2.40 and 2.26 (NCHMe$_2$), 0.78 (m, NCH(CH_3)$_2$).

Polymerization of Styrene. Runs 1−7: **4** and **5** (ca. 15 mg) and styrene (ca 3.7 g, 2000 equiv) were stirred for 2 days in CH_2Cl_2 (8 mL) at room temperature (runs 1 and 5), or in dichloroethane at 40 °C (runs 2 and 5), 60 °C (runs 3, 6, and 8), and 80 °C (runs 4 and 7). Evaporation of the solvent and unreacted styrene gave a white solid, which was isolated (run 2: 0.23 g, 6.3% yield; run 3: 0.37 g, 10% yield; run 4: 1.02 g, 28% yield; run 5: 0.07 g, 1.8% yield; run 7: 0.33 g, 9% yield; run 8: 0.93 g, 24% yield) and analyzed by GPC (THF). A representative ^1H NMR ($CDCl_3$) spectrum: 7.07 (br), 6.57 (br), 1.88 (br), 1.46 (br). A representative $^{13}C\{^1H\}$ ($CDCl_3$) spectrum: 145.3 (*ipso*-C), 128.1 (*o*- and *m*-C), 125.8 (*p*-C), 44.1 and 40.6 (alkyl chain). Run 8: Neutral complex **3** (10.0 mg, 0.0167 mmol), $NaBPh_4$ (28.6 mg, 0.083 mmol, 5 equiv), and styrene (3.48 g, 33.4 mmol, 2000 equiv) were mixed together in dichloroethane (5 mL) and stirred for 48 h at 80 °C. Evaporation of the solvent and unreacted styrene gave a gray solid, which was isolated (2.642 g, 76% yield) and analyzed by GPC (THF).

Polymerization of *N*-Vinylcarbazole. Complex **4** or **5** (ca. 11 mg) and *N*-vinylcarbazole (ca. 250 mg, 100 equiv) were stirred for 4 days in dichloroethane (2 mL) at room temperature or at 80 °C. Evaporation of the solvent left a light red solid consisting of unreacted *N*-vinylcarbazole (room-temperature experiments) or poly(*N*-vinylcarbazole) at >95% yield (80 °C experiments). Analysis by GPC (THF) indicated that the molecular weight of the polymer ranges between 23 725 and 367, with a maximum at 575 (reaction with **4**), or 2760 and 360, with a maximum at 433. These samples of poly(*N*-vinylcarbazole) were partially soluble in $CDCl_3$ and could be characterized by NMR spectroscopy (Chart 1).[31] ^1H NMR ($CDCl_3$): 8.1 (br, H5), 7.9 (br, H4), 7.6 (br), 7.3 (br, H7, H6), 6.6 (br, H3, H8, H2), 5.9 (br), 5.1 (br, H1), 3.7 (br), 2.4 (br), 2.0 (br), 1.8 (br), and 1.6 (br). $^{13}C\{^1H\}$ NMR ($CDCl_3$) 139.2 (C1a, C8a), 126.1 (C7, C2), 125.4 (C5a), 125.1 (C4a), 123.7 (C5), 123.4 (C4), 120.1 (C6), 118.9 (C3), 110.3 (C8), 110.1 (C1), 50.1, 48.1, 43.3.

Cyclic Voltammetry. Electrochemical measurements were performed on an Epsilon Electrochemical Analyzer using CH_3CN solutions of the nickel(II) complexes (0.002 M) and *n*-Bu_4NPF_6 (0.1 M). Cyclic voltammograms were obtained in a standard, one-compartment electrochemical cell using a graphite-disk electrode as working electrode, a platinum wire as the counter electrode, and an Ag−$AgNO_3$ (0.01 M in CH_3CN)

(31) Karali, A.; Froudakis, G. E.; Dais. P. *Macromolecules* **2000**, *33*, 3180.

reference electrode. The cyclic voltammetry was performed in the potential range −2.8 to 0.8 V using scan rates of 50−200 mV/s. Under these conditions, $E_{1/2}$ for the Fc^+−Fc couple is 90 mV.[32]

Reaction of [(η^3:η^1-IndCH$_2$Py)Ni(PPh$_3$)][BPh$_4$] (4) with PPh$_3$. Compound **4** (18 mg, 0.021 mmol) and PPh_3 (57 mg, 0.22 mmol, ca. 10 equiv) were dissolved in CD_2Cl_2 (0.75 mL), and ^1H and $^{31}P\{^1H\}$ NMR spectra were recorded 15 min later. The $^{31}P\{^1H\}$ NMR spectrum showed the signals of the starting material only ($\delta = 34.6$ ppm); the signal due to free PPh_3 was not detected. In the ^1H NMR spectrum, the only difference noted was the increase of the intensities of the signals for PPh_3. A second portion of PPh_3 (76 mg, 0.29 mmol, total of ca. 24 equiv) was added and the mixture analyzed by NMR. The $^{31}P\{^1H\}$ NMR spectrum showed the starting material ($\delta = 34.8$ ppm) along with a new broad peak at 9.4 ppm. No new peaks were detected in the ^1H spectrum, which showed the signals for **4** and PPh_3 (increased intensity). A last portion of PPh_3 (116 mg, 0.44 mmol, for a total of ca. 45 equiv) was added, and the spectra were recorded. The $^{31}P\{^1H\}$ NMR spectrum showed the starting material ($\delta = 34.9$ ppm) and a broad peak at −0.5 ppm. The ^1H NMR spectrum was as for the previous mixture. The anticipated AB signals (^{31}P) were not detected, implying that the complex [(η^3:η^0-IndCH$_2$Py)Ni(PPh$_3$)$_2$]$^+$ did not form.

[(η^3:η^0-Ind(CH$_2$)$_2$NC$_4$H$_8$)Ni(PPh$_3$)$_2$][BPh$_4$] (8) in Equilibrium with 5. Compound **5** (12 mg, 0.015 mmol) and PPh_3 (14 mg, 0.054 mmol, ca. 3.7 equiv) were mixed together in $CDCl_3$ (0.65 mL) and analyzed by ^1H and $^{31}P\{^1H\}$ spectroscopy 15 min later. The emergence of the new product **8** was evident from the $^{31}P\{^1H\}$ NMR ($CDCl_3$) spectrum: 36.1 ppm (d, $^2J_{P-P} = 26.8$ Hz) and 31.9 (d, $^2J_{P-P} = 26.8$ Hz). ^1H NMR ($CDCl_3$): 7.6−6.9 (PPh_3, BPh_4, Ind), 6.46 (H2), 6.35 and 6.02 (H4/H7), 4.89 (br, H3), 2.6−1.1 (signals for the tether overlapping with those of **5**). A 0.34:1 ratio of **8**:**5** was determined on the basis of the integration of the $^{31}P\{^1H\}$ NMR signals. Additional PPh_3 (20 mg, 0.077 mmol) was added to the sample, and the NMR spectra were recorded 15 min later, showing a 0.71:1 ratio. A final portion of PPh_3 (25 mg, 0.095 mmol) was added and the mixture analyzed by NMR spectroscopy, which showed a 1.48:1 ratio. The equilibrium constant has been calculated: $K_{eq} = 4.2 \pm 0.4$.

[(η^3:η^0-IndCH$_2$Py)Ni(dppe)][BPh$_4$] (9). Compound **4** (13 mg, ca. 0.015 mmol) and bis(diphenylphosphino)ethane (dppe, 19 mg, ca. 0.048 mmol, 3 equiv) were dissolved in CD_2Cl_2, and the sample was analyzed by NMR after 2 h. The $^{31}P\{^1H\}$ NMR spectrum showed free PPh_3 and free dppe along with two broad signals at 67.7 and 70.8 ppm. ^1H NMR (CD_2Cl_2): 7.6−6.7 (dppe, PPh_3, BPh_4, H5 to H7, py), 6.64 (d, $^3J_{H-H} = 7.3$ Hz, H4 or H7), 6.34 (H2), 5.96 (d, $^3J_{H-H} = 7.8$ Hz, H4 or H7), 5.47 (H3), 3.25 and 3.08 (d, $^2J_{H-H} = 14.2$ Hz IndCH_2), 2.08 (CH_2P).

[(η^3:η^0-Ind(CH$_2$)$_2$NC$_4$H$_8$)Ni(dppe)][BPh$_4$] (10). Compound **5** (11 mg, ca. 0.013 mmol) and bis(diphenylphosphino)ethane (dppe; 15 mg, 0.039 mmol, ca. 3 equiv) were dissolved in CD_2Cl_2, and the sample was analyzed by NMR after 2 h. The $^{31}P\{^1H\}$ NMR spectrum showed free PPh_3 and free dppe along with two broad signals at 68.4 and 65.3 ppm. ^1H NMR (CD_2Cl_2): 7.6−6.7 (dppe, PPh_3, BPh_4, H5 to H7, py), 6.56 (d, $^3J_{H-H} = 7.8$ Hz, H4 or H7), 6.03 (H2), 5.93 (d, $^3J_{H-H} = 8.2$ Hz, H4 or H7), 5.31 (H3), 2.49, 2.38, and 2.29 (NCH$_2$CH$_2$), 2.11 (free dppe), 1.72 (CH_2P).

Reaction of [(η^3:η^1-IndCH$_2$Py)Ni(PPh$_3$)][BPh$_4$] (4) with Pyridine. Compound **4** (29 mg, 0.034 mmol) and pyridine (10.9 μL, 0.14 mmol, ca. 4 equiv) were dissolved in CD_2Cl_2 (0.75 mL), and the sample was analyzed by NMR after 15 min. The $^{31}P\{^1H\}$ NMR spectrum showed the broadening of the signal of **4** (34.6 ppm). The addition of three portions of pyridine (for a total of 8, 16, and 24 equiv) led to further broadening of the signal of **4** until it disappeared and gave rise to the signal for free PPh_3. All the volatiles were then removed under vacuum and the $^{31}P\{^1H\}$ NMR spectrum was recorded, which showed that the main phosphorus-containing species is PPh_3 and implied the decomposition of **4**.

[{η^3:η^0-Ind(CH$_2$)$_2$N(C$_4$H$_8$)}Ni(PPh$_3$)(Py)][BPh$_4$] (11) in Equilibrium with 5. Compound **5** (29 mg, 0.034 mmol) and pyridine (5.5 μL, 0.068 mmol, 2 equiv) were dissolved together in $CDCl_3$ (0.75 mL), and the ^1H and $^{31}P\{^1H\}$ NMR spectra were recorded 15 min later. $^{31}P\{^1H\}$ NMR ($CDCl_3$): 32.1 ppm. ^1H NMR ($CDCl_3$): 7.6−6.9 (PPh_3, BPh_4, Ind), 6.60 and 6.52 (H4/H7), 6.28 (H2), 4.18 (br, H3), 2.79 and 2.55 (IndCH_2CH_2), 2.4 (m, NCH_2), 1.73 (NCH$_2$CH_2). On the basis of the integration of the $^{31}P\{^1H\}$ NMR signals a 2.3:1 ratio was established for the complexes **11** and **5**. An additional equivalent of pyridine (2.3 μL, 0.034 mmol) was then added to the above sample, and the NMR spectra were recorded 15 min later, which showed a 4.3:1 ratio of **11** and **5**. Repeated addition of 1 equiv of pyridine allowed the determination of the equilibrium constant: $K_{eq} = 33 \pm 4$. Evaporation of the solution to dryness re-formed the starting complex **5**.

Acknowledgment. The Natural Sciences and Engineering Research Council of Canada, le fond FCAR of Quebec, and the University of Montreal are gratefully acknowledged for financial support. W. Baille and Prof. J. Zhu are thanked for help with the GPC analyses, and F.-G. Fontaine is thanked for help with the electrochemistry experiments. Prof. M. C. Baird is thanked for valuable discussions on the relevance of carbocationic pathways in the polymerization reactions promoted by our complexes.

Supporting Information Available: Complete details on the X-ray analysis of **1** and **4**, including tables of crystal data, collection, and refinement parameters, bond distances and angles, anisotropic thermal parameters, and hydrogen atom coordinates. This material is available free of charge via the Internet at http://pubs.acs.org.

OM030241Q

(32) Pavlishchuk, V. V.; Addison, A. W. *Inorg. Chem. Acta* **2000**, *298*, 97.